

## FORMABILITY OF MAGNESIUM SHEET ZE10 AND AZ31 WITH RESPECT TO INITIAL TEXTURE

Lennart Stutz<sup>1</sup>, Jan Bohlen<sup>1</sup>, Dietmar Letzig<sup>1</sup>, Karl Ulrich Kainer<sup>1</sup>  
<sup>1</sup>GKSS-Forschungszentrum Geesthacht GmbH; Max-Planck-Straße 1; Geesthacht, D-21502, Germany

Keywords: Formability, magnesium sheet, forming limit, texture, dynamic recrystallisation

### Abstract

The commercial application of magnesium alloy sheets is hindered by their low formability and therefore technological and economic constraints. Tailoring the texture has been identified as playing a major role in enhancing the formability of magnesium sheets. In this study, the formability of magnesium sheet ZE10 and AZ31 was investigated. While the texture of AZ31 is of unfavourable basal type, ZE10 shows a significantly different texture with the basal planes being randomly distributed. More basal planes are oriented favourably for basal slip, promising higher formability and thus, lower process temperature. Formability is assessed by means of forming limit diagrams as a representation of material response to various strain paths. Nakajima tests were carried out from room temperature to 250°C. Local strain data is correlated with the microstructural evolution. This study reveals a significant influence of texture on formability with ZE10 sheet showing superior formability compared to AZ31.

### Introduction

Applying magnesium sheets in lightweight design bears a significant weight saving potential [1, 2]. Substitution of conventional materials, such as aluminium and steels, can help to reduce vehicle weight and thus, greenhouse gas emission and fuel consumption. Conventional sheets of alloys such as AZ31 show limited formability at low temperature which poses a serious obstacle to commercial applications. Distinct basal textures are formed during the rolling process and hamper the ability to strain hardening which is a prerequisite for improved formability [3]. For deformation in the thickness direction, the majority of basal planes are oriented unfavourably. To realise strain in thickness direction and thus in  $\langle c \rangle$  direction of the majority of grains, twinning and  $\langle c+a \rangle$  pyramidal slip are other options. While the former can only accommodate a low degree of plastic deformation, the latter is thermally not activated below 225°C in pure magnesium. Thus, forming components from magnesium sheets with typical basal type texture requires elevated process temperatures which results in high production costs.

Sheets such as ZE10 or ZW41 with weaker texture were reported to show generally superior formability [4-8] or competitive formability at lower process temperature. This study assesses the formability of two magnesium sheets with significantly varied texture, AZ31 representing a conventional sheet of typical basal type texture and ZE10 with a much more weak texture.

### Material and Experimental Procedures

The forming behaviour of magnesium sheets (thickness 1.5mm) of two different alloys was investigated. Conventional AZ31-B (Mg-3Al-1Zn-Mn) sheet and sheet of alloy ZE10 (Mg-1Zn-Ce-La-Zr) were received in annealed condition. The initial microstructure shows a recrystallised microstructure consisting of equiaxed grains with an average grain size of 10 - 11  $\mu\text{m}$  for both

cases, see figures 1 and 2. It is notable that ZE10 shows a higher contrast between different grains compared to AZ31. This implies that the orientation of grains differs more in ZE10 than in AZ31.

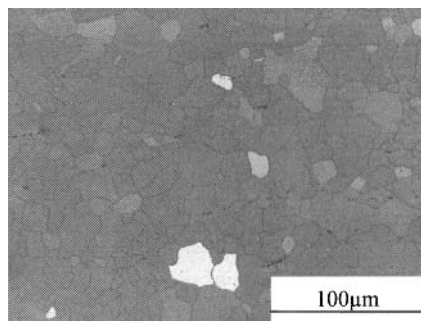


Figure 1: Microstructure of AZ31 sheet

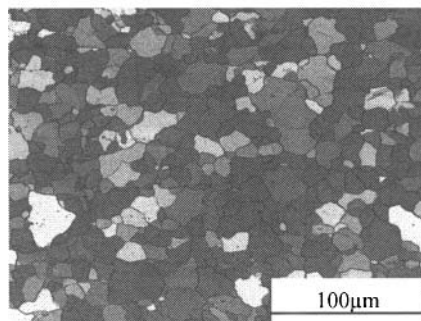


Figure 2: Microstructure of ZE10 sheet

Pole figures of the sheets were measured by a Panalytical X-ray diffractometer setup using  $\text{Cu K}\alpha$  radiation (40kV, 40mA). The resulting texture is presented as a recalculated (0002) pole figure from the orientation distribution function in figures 3 and 4. The measured distribution of basal planes differs significantly. AZ31 shows a typical texture of basal type where most grains are aligned parallel to the sheet plane. The angular spread of the orientation distribution is slightly broader to the rolling direction than to the transverse direction. This type of texture is typical for hot rolled magnesium sheets.

In contrary, the basal poles of ZE10 sheet are distributed more randomly. Furthermore, the maximum intensity is found at around 45° towards the transversal direction as a spread double peak. The overall distribution of basal planes is spread towards the transversal direction. Such a texture implies that more basal planes are oriented favourably for basal slip when loaded in sheet plane, promising higher formability.

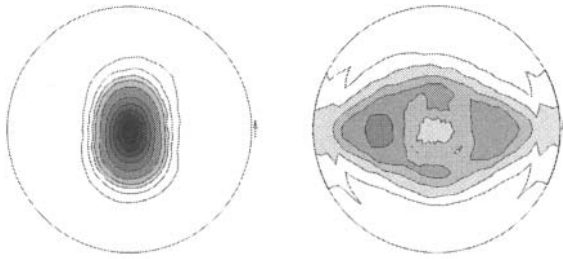


Figure 3: 0002 pole figure of AZ31 sheet,  $I_{\max} = 14.6$  m.r.d. Figure 4: 0002 pole figure of ZE10 sheet,  $I_{\max} = 3.6$  m.r.d.

Nakajima type tests were conducted, using an Erichsen 145-60 sheet metal testing machine. A hemispherical punch deformed the sheets at a speed of 1mm/s until fracture. Punch displacement and punch force were recorded digitally at a rate of 5Hz. The blank holder force was 400kN. Oiled PTFE foil of 0.05mm thickness was used as lubricant. Hasek type specimens [9], manufactured by water jet cutting, covered various strain paths from biaxial stretching over plane strain to deep drawing, refer to figure 5. All specimens were cut along the rolling direction. For each geometry and testing temperature, three specimens were tested. Tests were conducted at room temperature, 150°C, 200°C and 250°C respectively. All involved components of the testing device were heated to isothermal condition before testing. The use of an optical deformation measuring system ARAMIS allowed in situ strain measurements. A statistical pattern was applied on the sheet surface and high resolution pictures were recorded digitally during the tests at a rate of 12Hz. From the calculated strain data, forming limit curves according to ISO 12004 as well as strain path plots, were derived in the forming limit diagram (FLD). The FLD, as introduced by Keeler [10] is a powerful tool to assess the formability of sheets. The major strain as highest local strain in sheet plane is plotted versus the perpendicular local minor strain. Figure 5 shows a schematic FLD, specific strain paths are highlighted. At the onset of necking, severe localisation of strain, the so called forming limit curve is plotted.

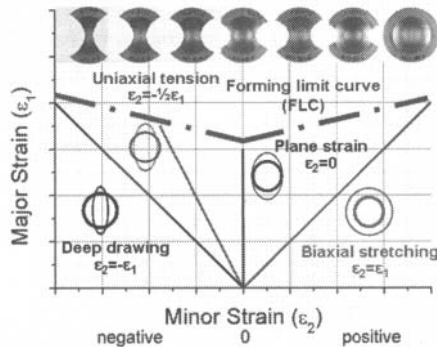


Figure 5: Schematic forming limit diagram. Hasek type specimens cover various strain paths.

Micrographs of the microstructure of deformed sheets were taken, using standard preparation techniques based on picric acid etching [11]. Samples were cut from the deformed specimen close to the crack location. The micro sections were grinded with SiC sandpaper and polished with SiO<sub>2</sub> suspension. Observation direction for all micrographs was the transversal direction (TD).

## Results

The mechanical response of the sheets is plotted as punch force – punch displacement curves in figure 6 for AZ31 and 7 for ZE10. For both sheets, specimens are shown that represent the outermost edges of the FLD. While the specimens marked with squares are deformed by biaxial stretching and thus, show a positive minor strain, the specimens marked with triangles represent specimens with negative minor strain. As a general tendency the specimens with positive minor strain require higher punch forces compared to their counterparts with negative minor strain. This can easily be explained by the larger area of contact and thus, amount of deformed material. In the case of AZ31, specimens tested at room temperature and specimens with negative minor strain tested at 150°C show an abrupt drop in punch force upon fracture of the specimens. The specimen tested at room temperature fracture at comparable low forces. All other specimens show a curve that can be separated in four segments: after an initial increase in punch force, a linear relationship between punch force and punch displacement is observed. The slope of this linear relationship decreases with increasing temperature and is generally higher for specimens with positive minor strain (biaxial stretching). Following up, a plateau force is reached and maintained until a rather sudden drop in punch force. The plateau is associated with diffuse necking of the specimen while the latter drop in force is due to crack initiation. It is notable that while the maximum punch displacement, the limiting dome height, increases with temperature in the case of biaxial stretching, the maximum limiting dome height is reached at 200°C for specimens with negative minor strain followed by a decrease of maximum punch displacement at 250°C.

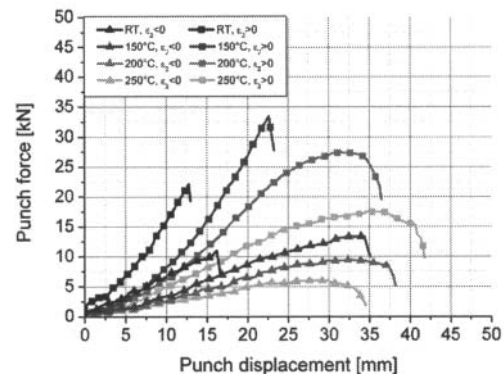


Figure 6: Punch force – punch displacement diagram for AZ31

In comparison, ZE10 shows simpler trends. Only specimen tested at room temperature show a brittle behaviour. With increasing temperature, the necessary punch force decreases and maximum punch displacement – the maximum dome height – increases. For biaxially stretched specimens, only slight differences in maximum dome height are achieved with increasing temperature from 150°C to 250°C. The limiting dome height of specimens with negative minor strain is always below their biaxially stretched counterparts. It is noteworthy that the maximum punch forces of biaxially stretched ZE10 are generally much higher than the punch forces of AZ31 specimens at the same temperature.

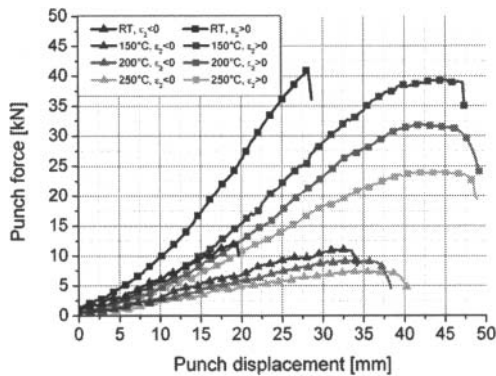


Figure 7: Punch force – punch displacement diagram for ZE10

By evaluation of the strain measurements as obtained by the ARAMIS system, the strain response of the material in terms of major strain vs. minor strain can be plotted in the FLD. Figures 8 and 9 show the strain response of both sheets until fracture of the specimens. For all tested specimens, there is an approximately linear relationship between minor and major strain. Deviations from this linearity are found at high values of major strain, close to fracture of the specimens.

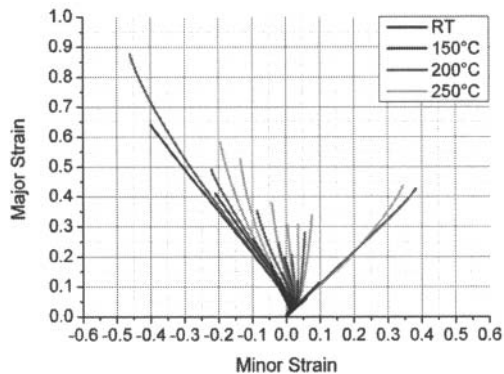


Figure 8: Strain paths of ZE10 sheet, testing temperature RT to 250°C

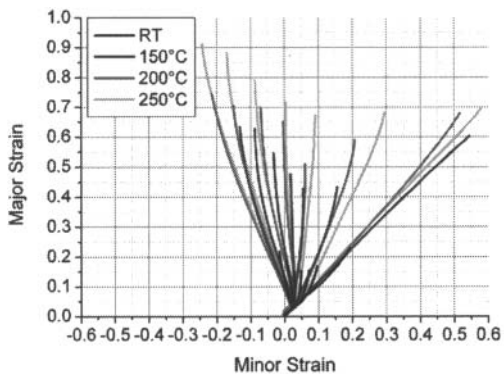


Figure 9: Strain paths of ZE10 sheet, testing temperature RT to 250°C

As a matter of tendency it is found that achieved values of major strain are higher for ZE10 than for AZ31. However, especially on the left hand side of the FLD, the slope of the measured strain paths is generally steeper for ZE10 than for AZ31. While for ZE10 it is found that an increase in temperature results in higher values of maximum major strain, AZ31 shows an exception from the rule at the outermost left side of the FLD. As already reported for the maximum dome height, maximum formability is reached at 200°C here and the strain path of specimens, tested at 250°C, does not even reach the maximum major strain as measured at 150°C.

Forming limit curves of the sheets according to ISO 12004 are shown in figures 10 and 11. The forming limit curve approximates the onset of necking of the material, beyond, strain localisation takes place until fracture. For AZ31, room temperature formability turns out to be poor. An increase of testing temperature to 150°C leads to a significant increase in formability under strain paths of negative minor strain, but gain in the domain of positive minor strain is low. Significant increase in stretch formability is found when increasing the test temperature to 200°C and beyond. The maximum major strain is reached with specimen tested at 200°C under negative minor strain. This result corresponds with the already observed findings in punch force – punch displacement curves and strain paths. The minimum major strain is found for specimen with minor strain close to zero, regardless of the temperature. This is a typical finding for sheet metals, the corresponding major strain value is commonly denoted  $FLD_0$ . For AZ31,  $FLD_0$  increases with temperature from 0.10 at room temperature to 0.27 at 250°C.

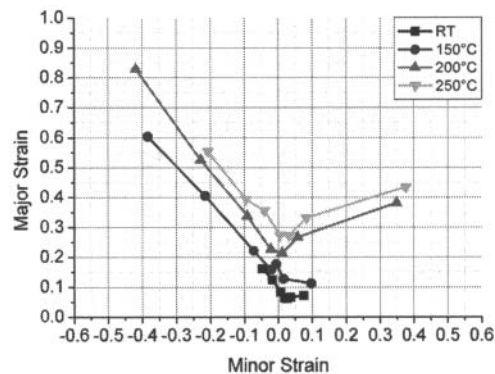


Figure 10: Forming limit curves of AZ31 sheet, testing temperature RT to 250°C

The forming limit curves of ZE10 sheet from room temperature to 250°C, as presented in figure 11, show generally higher values of major strain compared with AZ31. At room temperature formability is already higher than for AZ31 at 150°C under biaxial stretching.  $FLD_0$  depends strongly on temperature, showing an increase from 0.14 to 0.53 from RT to 250°C. ZE10 generally outperforms AZ31 in terms of formability. At 150°C, competitive formability can be achieved, the degree of deformation under plane strain condition and biaxial stretching is unmatched by AZ31 even at 250°C. Figure 11 confirms that formability under positive major strain does not increase significantly from 150°C to 250°C, for negative minor strain and plane strain condition a certain gain in formability is notable.

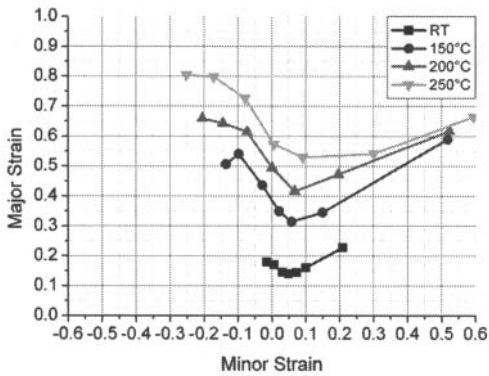


Figure 11: Forming limit curves of ZE10 sheet, testing temperature RT to 250°C

The microstructure of tested specimens is shown in figures 12 and 13. The micrographs show the microstructure close to the crack location. Figure 12a shows clearly that twins are formed during deformation of an AZ31 specimen with negative minor strain at room temperature. Twinning can contribute to the overall deformation of hcp material. Dynamic recrystallisation takes place at elevated temperatures. For the same strain path, figure 12b shows a specimen, deformed at 200°C. A duplex structure of fine,

recrystallised grains at the former grain boundaries of large, unrecrystallised grains is found. Figure 12c shows a similar structure, however, the fine grains at the former grain boundaries are larger. Under biaxial stretching, fewer twins are found at room temperature, figure 12d. At elevated temperatures, dynamic recrystallisation is initiated, at 200°C the microstructure is partially recrystallised and voids have formed in the material, figure 12e. Figure 12f shows a fairly recrystallised microstructure of a specimen, tested at 250°C under a strain path with positive minor strain (biaxial stretching). The microstructure consists of small grains, much smaller than the initial grain size.

ZE10 shows a different behaviour. At room temperature, fewer twins are formed as shown in figure 13a. At elevated temperatures, no evidence of dynamic recrystallisation can be found under a strain path with negative minor strain, see figures 13b and 13c. Instead, stretched unrecrystallised grains are found, forming a pan cake like microstructure. Under positive minor strain, severely deformed microstructure can be observed in the vicinity of the crack location, see figures 13d-f. Twins obviously play no role for the deformation under this strain path at elevated temperatures. Only at room temperature, very few twins can be observed in the microstructure, see figure 13d. With increasing temperature, the degree of elongation of the grains increases. At testing temperature of 250°C, individual grains are hard to identify, the microstructure consists of very flat, stretched grains.

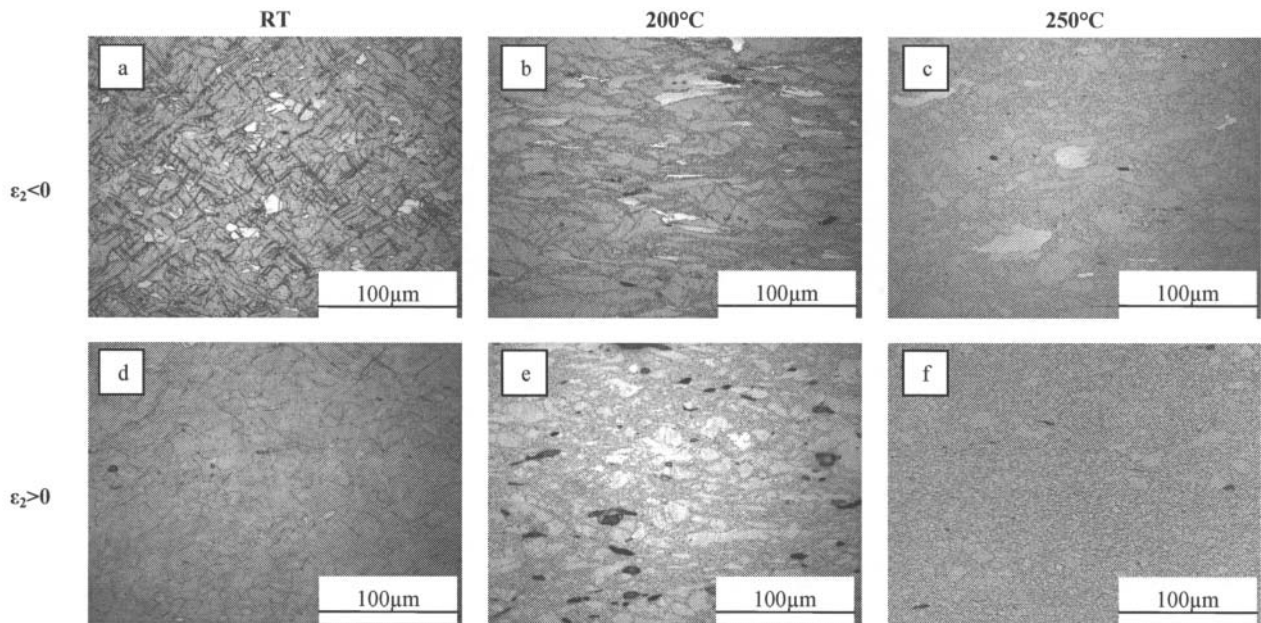


Figure 12: Micrographs of AZ31 sheet, tested at RT, 200°C and 250°C, negative minor strain (a-c) and positive minor strain (d-f)

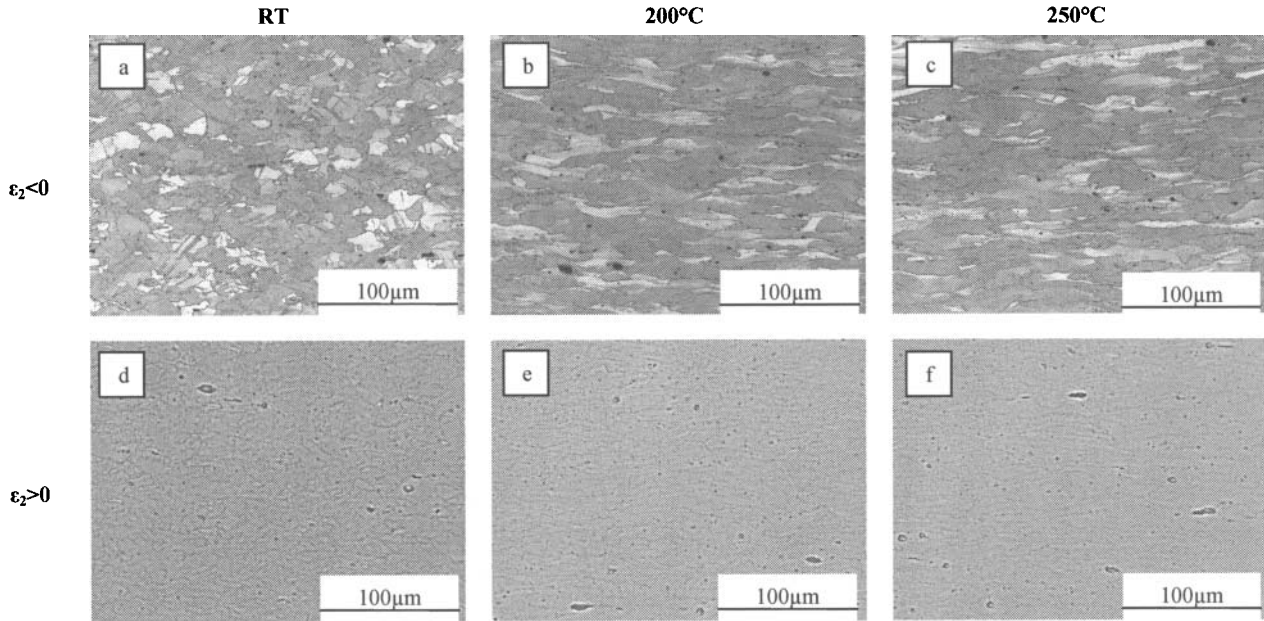


Figure 13: Micrographs of ZE10 sheet, tested at RT, 200°C and 250°C, negative minor strain (a-c) and positive minor strain (d-f)

### Discussion

The punch displacement - punch force curves of the both materials provide a first impression on the superior formability of ZE10 compared to conventional AZ31 sheet. It is notable that the limiting dome height and the achieved maximum major strain in the forming limit curves are in good, yet qualitative agreement. High limiting dome height equals good formability in the FLD as reported by Dreyer et al. [4]. The significant differences in strain response of the two sheets are mainly determined by their difference in texture. It is well known that a less pronounced texture can result in an overall higher formability of magnesium sheets [4-8]. The commonly found basal type texture of AZ31 basically does not favour basal slip as a result of the orientation even if a low CRSS favours it in comparison to other slip mechanisms. The deformation via this main slip system is hampered for all strain paths. In case of uni-axial tension tests this was confirmed by Agnew [12]. Strain in thickness direction and thus, perpendicular to the majority of basal planes, is difficult to realise at low temperatures. Twinning can only accommodate low degrees of plastic deformation in  $\langle c \rangle$  direction, formability of AZ31 at room temperature turns out to be poor. At elevated temperatures of 200°C and above, activation of pyramidal  $\langle c+a \rangle$  slip can compensate for the unfavourable orientation of basal planes, with increasing temperature, formability of AZ31 rises significantly especially for strain paths with negative minor strain. Under these strain paths, increasing deformation can be achieved up to 200°C. Interestingly, a further increase of temperature does not lead to a further increase in deformation but to a decrease. This indicates that a consideration of the activity of slip modes does not cover all aspects that are involved. ZE10 shows generally higher formability at any testing condition. The texture is much weaker and many basal planes are oriented favourably for basal slip.  $\langle a \rangle$  slip can be activated much more easily and can realise higher deformation compared to AZ31 under any strain path. In

summary, it can be considered that differences in the activation of deformation mechanisms are related to the texture of the material and that the main reason for the higher formability of ZE10 compared to AZ31 is the weaker texture. This is also concluded by Bohlen et al. [6] where the main features of uni-axial tensile tests were modelled based on the different textures rather than based on significant differences in critical stresses required for respective deformation mechanisms. Figures 12a-c reveal one specific feature which changes in the case of AZ31 if the temperature increases. Starting from a deformed microstructure at room temperature there is a considerable formation of necklace type structures of small recrystallised grains. It is noteworthy that this formation, which is observed after fracture of the samples, is visible up to tests at 200°C whereas higher temperatures lead to considerable grain growth. This behaviour was reported before [13, 14] and can explain highly localised deformation in the fine recrystallised grains between the stretched, unrecrystallised grains. At 250°C, the grains highly ductile zones are not observed anymore due to grain growth. In case of ZE10 the finding is different where no hint of ongoing recrystallisation is observed in this sheet. It is described that rare earth containing magnesium alloys generally show hampered dynamic recrystallisation [15, 16]. Furthermore, the texture of this sheet itself leads to changes in the activity of deformation mechanisms including a decrease of  $\langle c+a \rangle$  pyramidal slip activity. This also results in the delay of dynamic recrystallisation [5]. It is noteworthy that ZE10 shows superior formability especially under biaxial and plane strain conditions. The majority of failures in deep drawing processes happen under plane strain conditions. It should be pointed out that ZE10 shows superior formability under plane strain conditions at 150°C which is not surpassed by AZ31 even at 250°C.

## Summary and Conclusions

The present study proves the massive influence of texture on sheet formability of magnesium alloys. The alloy ZE10 shows superior formability, compared to the conventional alloy AZ31. This is illustrated by forming limit curves that cover various strain paths from deep drawing processes to biaxial stretching. At testing temperatures as low as 150°C, competitive formability can be achieved. Lowering the process temperatures in forming procedures such as deep drawing saves energy and cost as well as enables the use of less sophisticated lubrication systems and tools. With increased formability, component geometries can be realised that are currently restricted to very ductile materials such as mild steels or require complex forming processes such as super plastic forming. This study clearly proves that changing the texture of magnesium sheets can pave the way to commercial success of magnesium sheets by making forming processes less expensive or offering bigger process windows.

## Acknowledgement

The material used in this work is supplied by Salzgitter Magnesium Technology GmbH (SZMT) as part of the project "Mobile with magnesium". The authors appreciate this contribution by Dipl. Ing. Sebastien Wolff and Dr.-Ing. Peter Juchmann from SZMT and the financial support from the WING programme of the German Ministry of Education and Research (BMBF) under contract no. 03X3012H.

## References

1. B.L. Mordike, T. Ebert, "Magnesium Properties – applications – potential", *Materials Science and Engineering A*, 302 (2001), 37-45.
2. H. Friedrich, S. Schumann, "Research for a "new age of magnesium" in the automotive industry", *Journal of Materials Processing Technology*, 117 (2001), 276-281.
3. W.F. Hosford, R.M. Caddell, *Metal forming: Mechanics and Metallurgy*, (Upper Saddle River, NJ: PTR Prentice Hall, 1993) 68–79.
4. C.E. Dreyer, W.V. Chiu, R.H. Wagoner, S.R. Agnew, "Formability of a more randomly textured magnesium alloy sheet: Application of an improved warm sheet formability test", *Journal of Materials Processing Technology*, 210 (2010), 37-47.
5. S. Yi, J. Bohlen, F. Heinemann, D. Letzig, "Mechanical anisotropy and deep drawing behaviour of AZ31 and ZE10 magnesium alloy sheets", *Acta Materialia*, 58 (2010), 592-605.
6. J. Bohlen, M.R. Nürnberg, J.W. Senn, D. Letzig, S.R. Agnew, "The texture and anisotropy of magnesium–zinc–rare earth alloy sheets", *Acta Materialia*, 55 (2007), 2101–2112.
7. Y. Chino, K. Sassa, M. Mabuchi, "Texture and stretch formability of a rolled Mg–Zn alloy containing dilute content of Y", *Materials Science and Engineering A*, 513-514 (2009) 394-400.
8. E. Yukutake, J. Kaneko, M. Sugamata, "Anisotropy and Non-Uniformity in Plastic Behavior of AZ31 Magnesium Alloy Plates", *Materials Transactions*, 44 (2003), 452-457.
9. V. Hasek, " Untersuchung und theoretische Beschreibung wichtiger Einflußgrößen auf das Grenzformänderungsschaubild", *Blech Rohre Profile*, 25 (10) (1978), 493-499, 213-220, 285-292, 493-499, 613-627.
10. S.P. Keeler, "Plastic instability and fracture in sheet stretched over rigid punches", *ASM Transaction*, 56 (1964), 25-48.
11. V. Kree, J. Bohlen, D. Letzig, K.U. Kainer, " Metallographische Gefügeuntersuchungen von Magnesiumlegierungen", *Praktische Metallographie*, 41 (2004), no. 5: 233-246.
12. S.R. Agnew, "Plastic Anisotropy of Magnesium Alloy AZ31B Sheet", *Magnesium Technology 2002*, (Warrendale, PA: TMS, 2002), 169-174.
13. S.E. Ion, F.J. Humphreys, S.H. White, "Dynamic recrystallisation and the development of microstructure during the high temperature deformation of magnesium", *Acta Metallurgica*, 30 (10) (1982), 1909-1919.
14. J.A. del Valle, M.T. Pérez-Prado, O.A. Ruano, "Texture evolution during large-strain hot rolling of the Mg AZ61 alloy", *Materials Science and Engineering A*, 355 (2003), 68-78.
15. K. Hantzsche, J. Bohlen, J. Wendt, K.U. Kainer, S.B. Yi, D. Letzig, "Effect of rare earth additions on microstructure and texture development of magnesium alloy sheets", *Scripta Materialia*, 63 (2010), 725–730.
16. J. Bohlen, S. Yi, D. Letzig, K.U. Kainer, "Effect of rare earth elements on the microstructure and texture development in magnesium–manganese alloys during extrusion", *Materials Science and Engineering A*, 527 (2010) 7092–7098.